NASA TECHNICAL NOTE

NASA TN D-2711

NASA TN D-2711

EFFECTS OF IMPURITIES ON RADIATION DAMAGE OF SILICON SOLAR CELLS

by Joseph Mandelkorn, Lawrence Schwartz, Robert P. Ulman, Jacob D. Broder, Harold E. Kautz, and Richard Statler

Lewis Research Center
Cleveland, Ohio

NATIONAL AERONAUTICS AND SPACE ADMINISTRATION • WASHINGTON, D. C. • MARCH 1965

NASA TN D-2711

EFFECTS OF IMPURITIES ON RADIATION DAMAGE OF SILICON SOLAR CELLS

By Joseph Mandelkorn, Lawrence Schwartz, Robert P. Ulman, Jacob D. Broder, and Harold E. Kautz

Lewis Research Center
Cleveland, Ohio

and

Richard Statler

Naval Research Laboratory
Washington, D.C.

NATIONAL AERONAUTICS AND SPACE ADMINISTRATION

For sale by the Office of Technical Services, Department of Commerce,
Washington, D.C. 20230 -- Price $1.00

EFFECTS OF IMPURITIES ON RADIATION DAMAGE OF SILICON SOLAR CELLS*

by Joseph Mandelkorn, Lawrence Schwartz, Robert P. Ulman,
Jacob D. Broder, and Harold E. Kautz

Lewis Research Center

and

Richard Statler

Naval Research Laboratory
Washington, D.C.

SUMMARY

18215

Study of the effects of impurities on the characteristics of solar cells led to the conclusion that the impurity deliberately added to silicon in order to lower its resistivity also plays an important role in determining radiation-damage behavior and junction characteristics of cells. Cells made from silicon doped with aluminum to a resistivity of approximately 10 ohm-centimeters have superior characteristics and maximum power output in an atomic-radiation environment. The results obtained indicate that the use of 10-ohm-centimeter aluminum-doped cells in satellite power supplies will extend the lifetimes of such supplies in a radiation environment by a factor of 25.

INTRODUCTION

AUTHOR↑

Since the discovery of the Van Allen radiation belt in space and the high-altitude nuclear explosions of 1962, there has been concern about the useful life of solar-cell power supplies of satellites. The object of this report is to present information on a successful approach toward improvement of radiation-damage resistance, namely, the control of impurities in the silicon. The effects of some impurities on the radiation damage of silicon solar cells were described in reference 1, in which the study of radiation damage to boron-doped cells led to the conclusion that the boron atoms participated in the creation of recombination centers. In the work reported herein, the effect of other doping impurities on radiation damage was studied. In addition, modified cell-fabrication techniques were devised to improve cell characteristics and spectral response. By combining the best doping impurity and the best fabrication techniques, greatly improved cells were obtained.

EXPERIMENTAL RESULTS

Gadolinium atoms were substituted for boron atoms in the base region of n-on-p solar cells. Figure 1(a) shows a plot of base-region minority-carrier diffusion lengths as functions of 1-Mev electron dose for gadolinium-doped cells. Diffusion lengths for the cells were measured by the electron beam technique (ref. 1). The dose rate was 10^{11} 1-Mev electrons per square centimeter per second. Cell temperatures were held within 5° C of room temperature. The curve for 50-ohm-centimeter cells appears to be composed of three

*Presented at Fourth Annual Photovoltaic Specialists' Conference, Cleveland, Ohio, June 2-3, 1964.

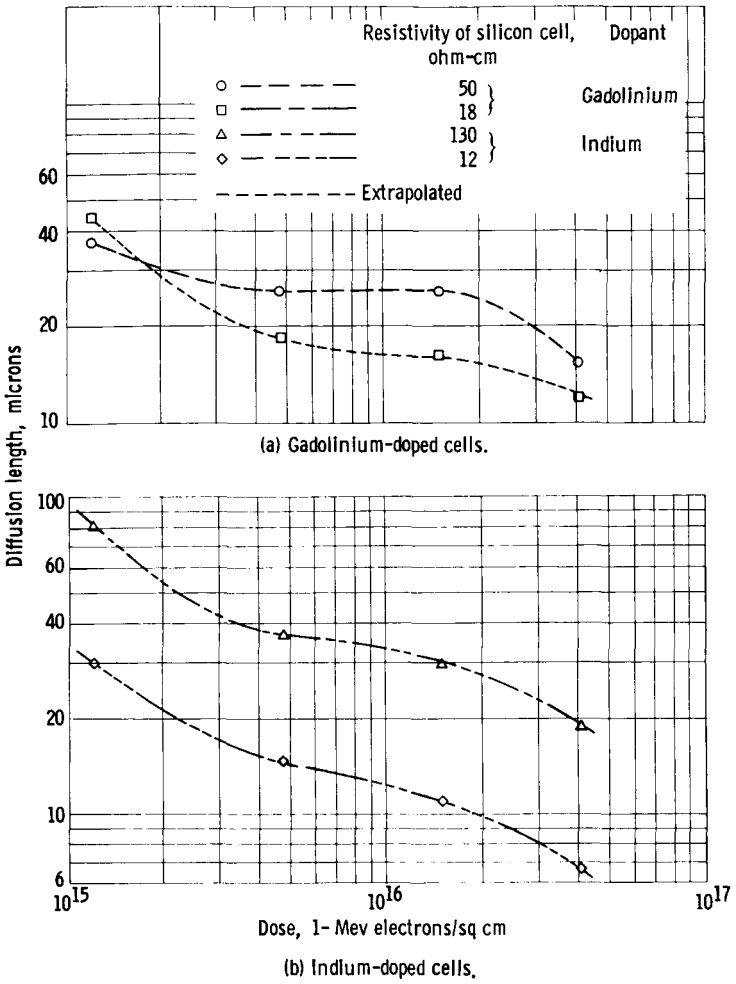

Figure 1. - Diffusion length as function of electron flux.

distinct regions. The central region of the curve in the dose range 4×10^{15} to 1.5×10^{16} 1-Mev electrons per square centimeter has a slope of zero. Vacancies in the cell material were definitely being generated in this dose range. Yet, there was no measurable change in base-region diffusion length or in cell short-circuit current. The other two regions of the curve differ from each other, as well as from the central region, in slope. It is emphasized that, for plots of the type shown, only the general shape and the values of diffusion length measured for specific doses are significant. The slopes between measured points have been assigned arbitrarily. The general shape of the curves suggests that the rate of introduction of damage is a function of bombardment dose, as well as impurity content.

The plot for the 18-ohm-centimeter cells has the same three-region appearance as that for the 50-ohm-centimeter cells. The central region has a small negative slope, however. At a dose of 1.2×10^{15} 1-Mev electrons per square centimeter, the diffusion length preserved in the 18-ohm-centimeter cells was higher than that in the 50-ohm-centimeter cells. This situation is not unusual. The gadolinium used to dope the 50-ohm-centimeter cell material was of lower purity than that used to dope the 18-ohm-centimeter cell material. Electrically inactive impurities are known to affect the formation of recombination centers in silicon (ref. 1). The density of recombination centers in solar cells of high-resistivity base material is strongly influenced by the concentration of electrically inactive impurities in the dose range that includes 10^{15} 1-Mev electrons per square centimeter. For higher dose ranges, the concentration of electrically active impurity, gadolinium in this case, dominates recombination-center formation. Thus, the 50-ohm-centimeter cells preserve longer diffusion lengths for doses above 4×10^{15} 1-Mev electrons per square centimeter.

Figure 1(b) shows the effects of bombardment on the diffusion lengths of 130- and 12-ohm-centimeter indium-doped cells. Again, the curves have a three-region appearance. The values of diffusion length preserved in the 130-ohm-centimeter cells far exceed those of the 12-ohm-centimeter cells for any specific bombardment dose. This behavior is similar to the damage behavior of 10-

and 100-ohm-centimeter boron-doped cells (ref. 1). The values of diffusion length preserved in the 130- and 12-ohm-centimeter indium-doped cells are, however, lower than those preserved in 100- and 10-ohm-centimeter boron-doped cells, respectively. There is, therefore, a dependency of rate of formation of recombination centers on the specific electrically active impurity element, as well as on its concentration.

Although not shown, the bombardment damage behavior of 5- and 12-ohm-centimeter gallium-doped cells results in similar three-region curves. Analysis of the curves for the various types of cells indicates that the slope of the central region increases with increasing concentration of electrically active impurity. A study is under way to obtain data on the behavior of bombarded 50-ohm-centimeter cells containing various dopants. It is expected that the completely flat region observed in the curve for the 50-ohm-centimeter gadolinium-doped cell in figure 1(a) will not occur for 50-ohm-centimeter boron-doped cells, whereas 50-ohm-centimeter aluminum-doped cells are expected to surpass the performance of the 50-ohm-centimeter gadolinium cells.

The relation between the diffusion length L retained in a bombarded semiconductor material and the total flux Φ of atomic particles can be expressed as $1/L^2 = 1/L_0^2 + K\Phi$. The damage constant K contains the various factors that determine the behavior of the sample material in its specific environment. Figure 2 is a plot of diffusion length against bombardment flux for various high-resistivity cells. None of the curves conform with the formula. This lack of conformity was first noted for high-resistivity boron-doped cells (ref. 1). The curve for the 20-ohm-centimeter boron-doped cell is shown as a straight line. The values of diffusion length for high-resistivity boron-doped cells show appreciable scatter, however, at a dose of 10^{15} 1-Mev electrons per square centimeter. The slope of any high-resistivity-cell curve is strongly dependent on electrically inactive impurity content in the dose range extending to 5×10^{15} 1-Mev electrons per square centimeter. The concentrations of electrically inactive impurities vary with purity of dopant source, material growth process, section of silicon ingot from which the wafer is cut, and cell fabrication process. Valid comparison of the effects of electrically active impurities on radiation damage can be made only at doses exceeding 5×10^{15} 1-Mev electrons per square centimeter. In this dose range, the superiority of aluminum-doped cells is evident from the plots shown.

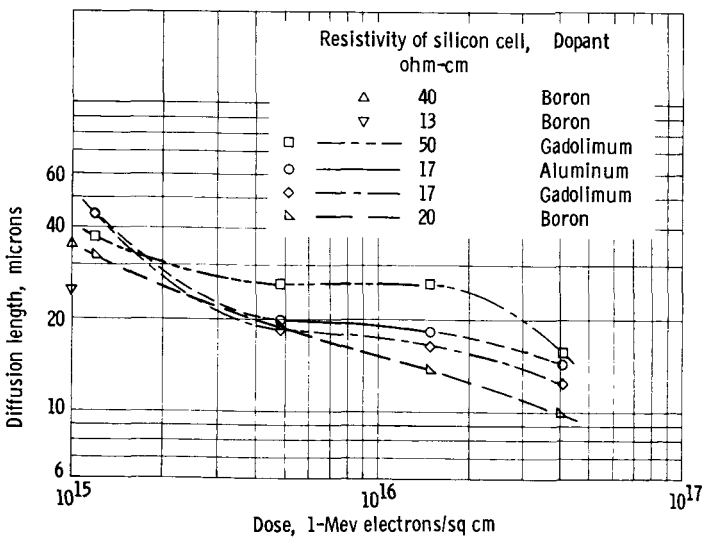

Figure 2. - Effects of impurities on postbombardment diffusion length.

The variability between types of cells is a result of impurities rather

TABLE I. - UNIFORMITY OF POSTBOMBARDMENT DIFFUSION LENGTHS OF SILICON SOLAR CELLS

Cell	Dose, 1-Mev electrons/sq cm			
	1.2×10^{15}	4.8×10^{15}	1.5×10^{16}	4.1×10^{16}
	Diffusion length, microns			
130-ohm-cm indium-doped cells				
8	83	36	29	18.4
9	83	36	29	18.5
10	78.5	36	30	18.9
11	80	37	29.5	18.7
17-ohm-cm aluminum-doped cells				
1	45.5	19.7	18.5	14.3
2	45.5	19.9	18.2	14.3
3	44.5	20.4	18.1	14.0
4	43	19.8	18.1	14.0
6	44.5	19.7	18.3	13.9
7	45.4	19.7	18.3	13.9

than the inconsistency of measurements, as shown in table I. Materials and processes were rigidly controlled for the cells shown. The result is good uniformity of diffusion lengths for each type of cell throughout an entire series of bombardments.

Figure 3 presents further data on the two types of cells considered in table I. The cells were bombarded, and their diffusion lengths were measured at Bell Telephone Laboratories. A definite decrease in the rate of introduction of recombination centers occurs for both the 130-ohm-centimeter indium-doped cells and the 17-ohm-centimeter aluminum-doped cells in the dose ranges 2×10^{14} to 8×10^{14} and 3×10^{15} to 1.2×10^{16} 1-Mev electrons per square centimeter. The fluxes at which diffusion lengths were measured at Bell Telephone Laboratories were slightly lower than those for the values of diffusion lengths shown in figures 1 and 2. The values of diffusion length determined from extrapolation of the points shown in figure 3 are in very good agreement with the data presented in table I. The change in the slope of the curves in the dose range 3×10^{15} to 1.2×10^{16} 1-Mev electrons per square centimeter would appear more pronounced if the plot had included values measured at 4×10^{16} 1-Mev electrons per square centimeter.

The bombardment behavior of lower-resistivity 1-ohm-centimeter cells is

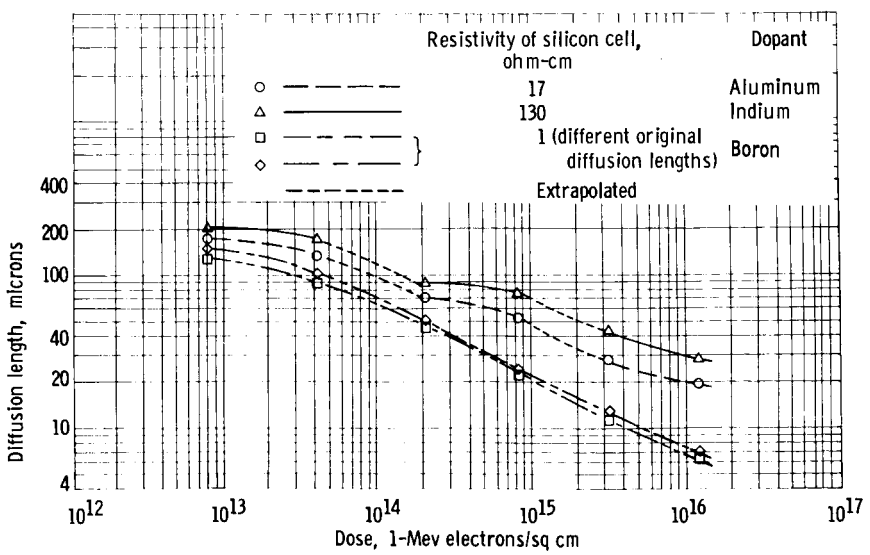

Figure 3. - Postbombardment diffusion length as function of electron flux.

shown at the bottom of figure 3. Two groups of these 1-ohm-centimeter cells having different values of unbombarded diffusion lengths are compared. After bombardment with a small dose of 10^{14} 1-Mev electrons per square centimeter, the differences in diffusion lengths preserved in each group are insignificant.

Unlike 1-ohm-centimeter cells, high-resistivity cells, which have larger values of original diffusion length, preserve their superiority to bombardment doses greater than 10^{15} 1-Mev electrons per square centimeter. Longer original diffusion lengths in high-resistivity cells are indicative of low concentrations of electrically inactive impurities in the base region of such cells. Consequently, the rate of introduction of recombination centers is slower in such high-resistivity cells even at doses that are equivalent to those that cells could experience after 1 year or more in the Van Allen belt. The preservation of long diffusion lengths in fabricated high-resistivity cells is therefore of significance in obtaining high-radiation-damage resistance in practical applications.

THEORY TO EXPLAIN EXPERIMENTAL OBSERVATIONS

From an analysis of the characteristics of modified cells, it was found that impurities influenced diffusion-length degradation, carrier-removal rate, open-circuit voltage, and junction characteristics of cells. It is impossible to predict characteristics of cells from mere knowledge of the resistivity of the base material. The following concepts are advanced to explain the experimental observations:

(1) Bombardment-generated vacancies are mobile at room temperature.

(2) Mobile vacancies may be captured by impurity atoms or other vacancies and may form impurity-vacancy or vacancy-vacancy configurations.

(3) Specific configurations so formed can have trapping-center or recombination-center behavior.

(4) Terminology for the variables involved in the formation of configurations involving capture of mobile vacancies can be patterned after carrier-capture terminology. Equations showing the relations of variables will also be similar to those for carrier capture. Variables are

(a) Specific impurity element, its electronic state, and its concentration in the lattice

(b) Concentration of generated mobile vacancies

(c) Localized lattice imperfections

(5) Types of configurations are impurity - single-vacancy, impurity - multiple-vacancy, and vacancy-vacancy clusters. The concentration of compound-vacancy configurations is significantly determined by the density of generated mobile vacancies, as well as the variables previously considered.

(6) When compound-vacancy configurations exist because of instantaneous local generation of high densities of mobile vacancies, redistribution occurs with time at room temperature.

On the basis of these concepts, it is possible to explain impurity effects on junction characteristics (ref. 1), changes in damage-introduction rate with bombarding-particle energy and with bombardment dose, differences between proton- and electron-damage introduction, and room-temperature annealing of proton-bombarded cells.

USE OF IMPURITY EFFECTS IN SOLAR-CELL DESIGN

The study of impurity effects has led to the design and fabrication of improved cells. With regard to the preservation of diffusion length in the base region of solar cells after bombardment, the optimum base-region material should contain the minimum achievable concentration of electrically active impurity. The power output of the solar cell, however, depends on the base-region parasitic resistance, as well as on the base-region diffusion length. Base-region parasitic resistance increases with decreasing electrically active impurity concentration. Furthermore, the open-circuit voltage of cells decreases with decreasing electrically active impurity concentration, while the temperature coefficient of power output increases (ref. 2). From investigation of these effects, it has been concluded that the optimum concentrations of electrically active impurity in solar-cell material correspond to material resistivities in the 10- to 20-ohm-centimeter range. In the past year, more than two hundred 10- to 20-ohm-centimeter solar cells (hereafter referred to as 10-ohm-cm cells) have been fabricated and analyzed at Lewis Research Center. As a result of this effort, the following important advantages stemming from use of 10-ohm-centimeter silicon for solar cells have become apparent.

Application advantages:

(1) Extremely shallow junction cells with very good junction characteristics have been made with excellent yields by using 10-ohm-centimeter silicon.

(2) These cells have better curve power factors, much higher short- and long-wavelength response, and higher efficiencies than 1-ohm-centimeter cells.

(3) Considerably higher long-wavelength response and higher efficiencies are preserved in bombarded 10-ohm-centimeter cells than in 1-ohm-centimeter cells.

(4) The 10-ohm-centimeter cell degradation with temperature is such that the 10-ohm-centimeter cell is still superior to the 1-ohm-centimeter cell at temperatures to 100° C.

Production advantages:

(1) Material rejection is low. Original minority-carrier lifetime in 10-ohm-centimeter material exceeds that preserved after subjecting the material to diffusion processing. This is usually not true for 1-ohm-centimeter material.

(2) Distributions of characteristics of 10-ohm-centimeter cells are tighter because of the superior properties of 10-ohm-centimeter material and because of the better and controllable junction characteristics attainable by using 10-ohm-centimeter material.

(3) Special low-cost superblue coatings can be applied to the 10-ohm-centimeter cell.

The benefits to be realized from the use of the 10-ohm-centimeter material and the characteristics of 10-ohm-centimeter cells justify application of such cells at temperatures to 100° C in nonradiation environments. In a radiation environment, the efficiencies preserved in 10-ohm-centimeter cells are sufficiently higher than those of 1-ohm-centimeter cells so that the 10-ohm-centimeter cell is definitely superior to the 1-ohm-centimeter cell in power output at 100° C (ref. 2).

ALUMINUM-DOPED CELL

Since the specific impurity element added to the silicon material to reduce its resistivity to the 10- to 20-ohm-centimeter range will influence all the characteristics of the cell, a study was made of the use of aluminum, indium, gallium, or boron for doping silicon in this resistivity range. The results show that aluminum is the most desirable impurity element (ref. 1).

Approximately 50 aluminum-doped 17-ohm-centimeter cells were fabricated. The characteristics of such cells are as follows:

Open-circuit voltage, v	0.54
Short-circuit current, ma	62 to 65
Area, sq cm	1.8
Minimum outer-space equivalent power output, mw	24
Minimum outer-space equivalent efficiency, percent	9.5
Curve power factor, percent	70
Outer-space current for 0.4- to 0.6-micron region of solar spectrum, ma	26
Ratio of outer-space current for 0.4- to 0.6-micron region to short-circuit current	0.4
Grid fingers	10
Thickness, in.	0.008 to 0.020
n value	<2
Diode reverse current for 0.6 v bias, μamp	<20
Contact resistance, ohms	0.25 to 0.4
Diffusion length, microns	150 to 200
Coating	superblue
Dopant	aluminum
Temperature coefficient, percent/°C	0.53

The cells are made by a standard diffusion process (ref. 3) at temperatures of approximately 800° C. The sheet resistance of the diffused layer must be kept at or below 200 ohms per square, and this determines the diffusion times, which are approximately 30 minutes. Ten grid fingers on the top surface of the cell

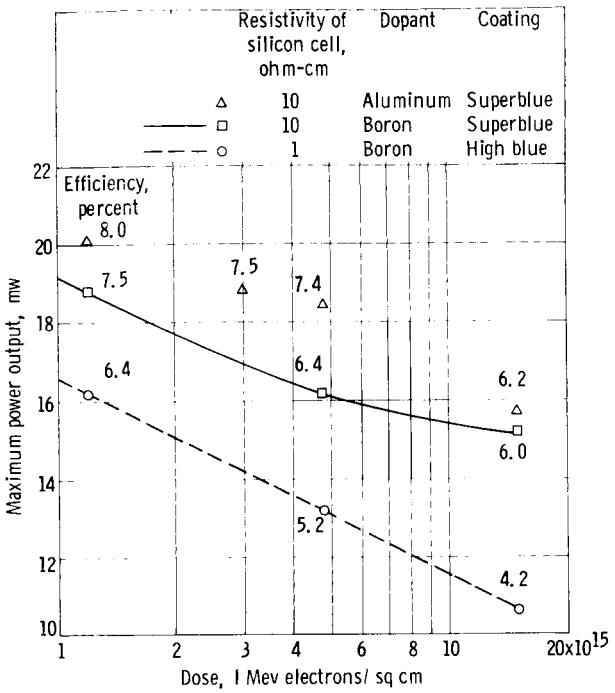

Figure 4. - Maximum power output as function of electron flux.

permit attainment of curve power factors of 70 percent for the maximum value of sheet resistance cited. Experiments revealed that the equivalent outer-space currents of these cells are not appreciably decreased for a base-region thickness of 0.008 inch. Depending on application requirements, the thicknesses of the cells can therefore range from 0.008 to 0.020 inch. Minority-carrier diffusion lengths of 200 microns are obtainable in fabricated cells of this type by using the optimized low-temperature diffusion process. The low-temperature short-time diffusions also result in extremely shallow junctions that have better junction characteristics and lower diode reverse currents than those obtained for deeper junctions in 1-ohm-centimeter material. In addition, the high short-wavelength response achieved, coupled with a special superblue antireflective coating, results in collecting 40 percent of the cell short-circuit current from the 0.4- to 0.6-micron region of the solar spectrum. The significance of this superblue characteristic in preserving the efficiency of the cells after bombardment is illustrated in reference 4. The high short- and long-wavelength collection of the cells results in their equivalent outer-space short-circuit currents being higher than those normally obtained for 1-ohm-centimeter cells despite the extra grids on the cell surfaces.

The open-circuit voltages of the cells are 0.54 volt, which is the common value of this parameter for 10-ohm-centimeter cells. The efficiencies for a 1.8-square-centimeter area (main contact subtracted) range from 9.5 to 10.5 percent. The spread in efficiencies is small because of the uniformity of long-wavelength collection under the solar spectrum, the reproducibly good junction characteristics, and the controls used in the fabrication process that are achievable by using 10- to 20-ohm-centimeter material.

PERFORMANCE OF BOMBARDED ALUMINUM-DOPED CELLS

From a series of bombardments of these aluminum-doped cells and of 1-ohm-centimeter high-blue and 10-ohm-centimeter superblue boron-doped cells, data were compiled on power outputs and efficiencies preserved after irradiation. The data are shown in figure 4. Power outputs and efficiencies were measured for the 1- and 10-ohm-centimeter boron-doped cells by using a filter-wheel simulator (ref. 4). Efficiencies are predicted for the aluminum-doped cells on the basis of measurements of initial characteristics and postbombardment diffusion lengths. Measurements of the short-circuit currents of these cells under the simulator were not possible at the time of bombardment. The aluminum-

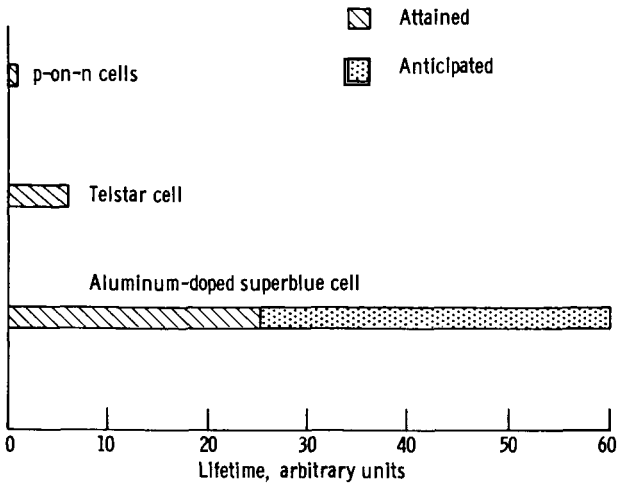

Figure 5. - Comparative lifetimes.

doped cells, however, were equal or superior to the 10-ohm-centimeter superblue boron-doped cells in all characteristics and preserved longer diffusion lengths after bombardment than did the 10-ohm-centimeter superblue boron-doped cells. The predictions are therefore believed to be reliable.

On the basis of approximately 12 bombardments of the cells with 10-Mev protons and a series of electron bombardments, approximations of anticipated lifetimes have been made for various types of cells in a Telstar I orbit and with Telstar 7 solar-cell shielding. An arbitrary lifetime of 1 has been assigned to the p-on-n cell in figure 5. The data of Waddell (ref. 5) and of Rosenzweig (ref. 6) of comparative damage of 1-ohm-centimeter p-on-n and n-on-p cells result in assignment of a comparative lifetime of six times that of the p-on-n cell for the 1-ohm-centimeter Telstar cell. Comparison of the data for the aluminum-doped superblue cells with the data for the Telstar-type cells results in assigning a factor of 25 times that of the p-on-n cell for the aluminum-doped superblue cell.

It must be emphasized that the full potential of the aluminum-doped superblue cell has not been realized as yet. The possibility of the inclusion of chlorine in aluminum-doped silicon, as well as the further elimination of detrimental electrically inactive impurities, could increase the comparative lifetime for the aluminum-doped superblue cell to as much as 60 times the p-on-n value.

CONCLUDING REMARKS

Modification of recombination theory must be made in order to account for the observed behavior of bombarded solar cells.

The study of impurity effects has led to the design of superior solar cells made from silicon containing aluminum. Such cells have shallower junctions, better junction characteristics, and broader spectral response than present industrial cells. The properties of the silicon base material, as well as the aforementioned characteristics, result in these cells having appreciably better performance in radiation environments. Furthermore, the use of 10-ohm-centimeter aluminum-doped silicon for fabrication of solar cells will result in higher production yields and closer tolerances on the characteristics of these cells.

Lewis Research Center
National Aeronautics and Space Administration
Cleveland, Ohio, September 28, 1964

REFERENCES

1. Mandelkorn, Joseph, et al.: Effects of Impurities on Radiation Damage of Silicon Solar Cells. Jour. Appl. Phys., vol. 35, no. 7, July 1964, pp. 2258-2260. (See also NASA TM X-52007.)

2. Broder, J., et al.: Solar Cell Performance at High Temperatures. Proc. Fourth Annual Photovoltaic Specialist's Conf., Inter Agency Advanced Power Group, IEEE, AIAA, and NASA Lewis. Cleveland (Ohio), June 2-3, 1964.

3. Mandelkorn, J., McAfee, C., Kesperis, J., Schwartz, L., and Pharo, W.: Fabrication and Characteristics of Phosphorous-Diffused Solar Cells. Jour. Electrochem. Soc., vol. 109, no. 4, Apr. 1962, pp. 313-318.

4. Mandelkorn, J.: A Filter Wheel Solar Simulator. Proc. Fourth Annual Photovoltaic Specialist's Conf., Inter Agency Advanced Power Group, IEEE, AIAA, and NASA Lewis, Cleveland (Ohio), June 2-3, 1964.

5. Waddell, R. C.: Radiation Damage to Solar Cells on Relay I and II. Proc. Fourth Annual Photovoltaic Specialist's Conf., Inter Agency Advanced Power Group, IEEE, AIAA, and NASA Lewis, Cleveland (Ohio), June 2-3, 1964.

6. Rosenzweig, W., Gummel, H. K., and Smits, F. M.: Solar Cell Degradation Under 1-Mev Electron Bombardment. Bell System Tech. Jour. vol. 42, no. 3, Mar. 1963, pp. 399-414.

NASA-Langley, 1965 E-2724